European Congress on Computational Methods
in Applied Sciences and Engineering (ECCOMAS 2012)
J. Eberhardsteiner et.al. (eds.)
Vienna, Austria, September 10-14, 2012

A MULTI-MESH ADAPTIVE SCHEME FOR AIR QUALITY MODELING WITH THE FINITE ELEMENT METHOD

Lluís Monforte, Agustí Pérez-Foguet*

Universitat Politècnica de Catalunya – BarcelonaTech, Laboratorio de Cálculo Numérico,
Departamento de Matemática Aplicada III, Jordi Girona 1-3, 08034, Barcelona, España.
lluis.monforte@upc.edu,agusti.perez@upc.edu*

Keywords: Adaptivity, Non-steady convection-diffusion-reaction equations, Nonlinear reaction model, Photochemical model, CB05, Computational cost

Abstract. *A multi-mesh adaptive scheme for convection-diffusion-reaction problems is presented. The proposal is applied to air quality modeling, especifically to the simulation of a pollutant punctual emissions. The performance of the proposal is analyzed with different nonlinear reaction models, including the photochemical model CB05 implmented within the Comunity Multiscale Air Quality model, which involves sixty-two species and very different characteristic reaction times. The problem is solved with splitting of transport and reaction processes. This allows to discretize the species in distinct computational meshes, adapted to the distribution of the error indicator of each case. A common reference mesh is used for all species and during all problem evolution. A remeshing technique based on imposing the volume of new elements is used to define and update the computational meshes. An error indicator well suited for problems involving large variation of the unknowns is used. A single-mesh strategy, with remeshing adapted to the most demanding specie in each part of the domain, is used for comparison. The results of the examples presented show that the accuracy of single and multi-mesh strategies are similar. Instead, computational cost of multi-mesh is lower than single-mesh in most cases. Reduction increases with the number of species and the number of plumes. An example of a punctual emissor in a three-dimensional domain, with realistic values of CB05 components, is presented.*

1 Introduction

Air quality modeling aims to represent all the processes that occur to pollutans in the atmosphere. These processes are modelized in a set of partial differential equations (PDEs). Traditionally, these PDEs are numerically evaluated in structured grids whose horitzontal resolution is in the order of few kilometers and the vertical resolution depends on altitude, finer near the ground level [22]. Some of the processes occur in smaller scales than the geometric resolution and they may not be well presented. For example, emissions of an industrial plant are diluted in a cell of a coarse grid and the details of the chemical interaction are lost because of the nonlinearity of the chemical reactions [9].

In order to decrease this source of uncertainly, adaptive schemes have been proposed in air quality modeing at local scale. In adaptive schemes, domain is discretized such that a mesure of the error is reduced. Various strategies have been presented. For example, in [28], the mesh is adapted moving the nodes of a structured, regular grid (r-adaptivity). The accuracy of small-scale plume structure near the source is higher than with a uniform static grid; however, the computational cost is several times larger with adaptivity, since both grids have the same number of nodes. Adaptivity strategy does not reduce the problem size in this case. This strategy has been merged with the Comunity Multiscale Air Quality (CMAQ) model [10]. On the other hand, in [29, 11], the mesh is updated inserting new nodes in the elements whose error is larger than a tolerance (h-adaptivity). The computational cost of the adaptive scheme is lower than that obtained with an uniform mesh, for the same accuracy. In both schemes, a dynamic adaptive scheme is used; the mesh is updated several times during the simulation. Instead, in [32] a nested grid aproach is proposed. A finer grid is defined in the interior of some cells of a coarse grid; the size of the coarse grid is an intenger multiple of the size of the fine grid. The solution of the coarse mesh is computed before the finer mesh and is used as initial conditions; the solution of the coarse mesh in the overlaped zone may be updated. Typically, the zone discretized with a finner mesh is defined a-priori. This last approach is not well suited for unstructured meshes.

Most of the adaptive schemes, as these referenced, solve the problem with a single and unique mesh for all species. However, the species may exhibit some qualitative differences: While some may be very smooth in all the domain and can be discretized with coarse meshes with accuracy, others may have big gradients in some regions of the domain and may need some refinement in it in order to decrease the error. In this kind of problems, involving a large number of unknowns with different spatial distribution, multi-mesh schemes can help. They have been used in a wide range of problems involving different unknwons. Every component of the solution is discretized in a different mesh, that can be independently adapted to the evolution of its reference component. In [14, 12], a multi-mesh approach is used for an optimal control problem and dentritic growth. In [26, 7, 27], several examples are solved using hp-adaptive Finite Element Mehtod with a multi-mesh approach. In [31], an example for dentritic growth and a detailed explenation of matrix assembling and elemental integration are presented. However, in all references, the number of unknowns is reduced, two or three, and a tree-like algorthm is used to refine the meshes.

In this work, we propose a multi-mesh adaptive scheme for convection-difussion-reaction equations, especifically for air quality modeling with realistic photochemical models, involving a large number of unknowns. Model is splitted in transport and reaction parts. Transport is decoupled beetwen species, and each one can be solved independently of the others. Mesh of each specie is adapted to the specific characteristics of its spatial distribution with a recently

proposed adaptive scheme [17]. Reaction is reduced to a set of differential equations involving all species, uncoupled node by node. Time-integration of reaction is computed at all nodes present in any mesh. With this approach, a tree-like discretization of the domain is not necessary because the solution is not couppled in a large system of linear equations. A set of numerical tests have been done for a point source emision problem using different chemical models involving different number of species. Computational cost of single and multi-mesh strategies are compared. An example of the punctual emission problem with a realistic set of values of CB05 components, varying in height, is presented to illustrate the practical application of the proposal. Values are provided by a simulation with the CMAQ model. CMAQ-CB05 implementation is merged with the convection-difussion-reaction model.

2 Mathematical and numerical model

Convection-diffusion-reaction equations descriving transportation of contaminants given a velocity field can be expressed as:

$$\begin{cases} \partial_t u_i + \mathcal{L}_i^t u_i - \mathcal{L}_i^r \mathbf{u} = 0 & \text{in } \Omega \times (0,T] \\ u_i(\mathbf{x},0) = u_{0i}(\mathbf{x}) & \text{in } \Omega \\ \mathcal{M} u_i = 0 & \text{in } \partial\Omega \times (0,T] \end{cases} \tag{1}$$

where u_i stands for the concentration of specie $i \in \{1,...,n_e\}$, n_e is the number of species, $\mathbf{u} \in \mathbb{R}^{n_e}$ is the vector of unknowns, $\Omega \subset \mathbb{R}^3$ is a bounded subset and $\mathcal{M}$ are the boundary conditions. Two diferential operators, $\mathcal{L}_i^t$ and $\mathcal{L}_i^r$, descrive transport and reactions:

$$\mathcal{L}_i^t u_i = \mathbf{a} \cdot \nabla u_i - \nabla \cdot (\mathbf{D}_i \cdot \nabla u_i) - s_i \tag{2a}$$

$$\mathcal{L}_i^r \mathbf{u} = r_i(\mathbf{u}) \tag{2b}$$

where $\mathbf{a}$ is the advective velocity, $\mathbf{D}_i$ is the diffusion coefficient tensor and $r_i(\mathbf{u})$ is the velocity of production due to chemical reactions and s_i is an optional source term. Functions are assumed sufficiently differentiable in all their variables.

Equation (1) defines a system of coupled partial differential equations (PDE). The solution of each component depends on all the others because of coupling in the reactive term. In air quality modeling, it is common to use an splitting strategy to separate all the physical and chemical processes that occur to the pollutants in the atmosphere [5, 3, 4]. Each process is evaluated with a specific numerical method designed for the particularites of each one. In this work, a second order Strang Splitting between transport and reaction is proposed. Let $\boldsymbol{\varphi}$ be a approximation of $\mathbf{u}$, and $\boldsymbol{\varphi}^i$, $i = 1,2,3$, approximations to $\boldsymbol{\varphi}$, then following steps are defined to time integrate the system of PDE from t_n to t_{n+1}:

1: Reactive Step

$$\partial_t \boldsymbol{\varphi}^1 = \mathcal{L}^r(\boldsymbol{\varphi}^1) \quad \text{for } [t_n, t_{n+1/2}],\ \boldsymbol{\varphi}^1(.,t_n) = \boldsymbol{\varphi}(.,t_n), \tag{3a}$$

2: Transportation Step, $\forall i \in \{1,...n_e\}$

$$\partial_t \varphi_i^2 + \mathcal{L}_i^t(\varphi_i^2) = 0 \quad \text{for } [t_n, t_{n+1}],\ \varphi_i^2(.,t_n) = \varphi_i^1(.,t_{n+1/2}), \tag{3b}$$

3: Reactive Step

$$\partial_t \boldsymbol{\varphi}^3 = \mathcal{L}^r(\boldsymbol{\varphi}^3) \quad \text{on } [t_{n+1/2}, t_{n+1}],\ \boldsymbol{\varphi}^3(.,t_{n+1/2}) = \boldsymbol{\varphi}^2(.,t_{n+1}) \tag{3c}$$

and setting:

$$\boldsymbol{\varphi}(.,t_{n+1}) = \boldsymbol{\varphi}^3(.,t_{n+1}). \tag{3d}$$

Equation (3b) defines a decoupled PDE, one PDE for each component of the solution. Equations (3a) and (3c) are still coupled PDEs. Equation (3b) defines the usual transportation (convection-difusion) equation. Any numerical scheme well suited for this problem can be used. In this work, we use the Finite Element Method. The solution of each specie is discretized in a different mesh $\mathcal{T}_i$:

$$u_i(\mathbf{x},t) \approx \varphi_i(\mathbf{x},t) = \sum_{j=1}^{ndf_i} \varphi_{i,j}(t) N_{i,j}(\mathbf{x}) \tag{4}$$

where $N_{i,j} \in V_h^i$ is the component j of the basis of functions of specie i, and V_h^i is the corresponding finite element space associated with the mesh $\mathcal{T}_i$, and ndf_i is the number of nodes of specie i. This aproximation is introduced in the weak formulation, equation (3b). A Least-Square stabilization tecnique and a Crank-Nicolson scheme are used (further details can be found in [6]). The resulting system of linear equations is solved with the Conjugate Gradient Method wih an incomplete Cholesky preconditioner [20, 15].

The reactive step, defined in equations (3a) and (3c), is couppled between all species. Introducing the weak formulation, the problem can be stated as: find $\boldsymbol{\varphi}$ such that:

$$\begin{cases} (\partial_t \boldsymbol{\varphi}, v) = (\mathbf{r}(\boldsymbol{\varphi}), v), & \forall v \in H^2(\Omega) \\ \boldsymbol{\varphi}(\mathbf{x}, t_n) = \boldsymbol{\varphi}_0(\mathbf{x}), & \text{in } \Omega \end{cases} \tag{5}$$

where $(\cdot,\cdot)$ is the inner product, v are the test functions of the solution space $H^2(\Omega)$ and $\partial_t \boldsymbol{\varphi} = \mathbf{0}$ in Γ_D is assumed. Since all species are not defined in the same mesh, formally, a new mesh, $\overline{\mathcal{T}} = \bigcup_{i=1}^{n_e} \mathcal{T}_i$, that contains all nodes of the set of meshes $\{\mathcal{T}_1, ..., \mathcal{T}_{n_e}\}$ is defined. The space of the solution associated to this new mesh, $\overline{V_h}$, contains all the spaces of the solutions associated to the meshes where the solution was defined; that is: $V_h^i \subset \overline{V_h}\ \forall i \in \{1, ..., n_e\}$. Solution is discretized as:

$$\boldsymbol{\varphi} = \sum_j \boldsymbol{\varphi}_j(t) \overline{N}_j(\mathbf{x}) \tag{6}$$

where $\overline{N}_j$ is the component j of the basis function of $\overline{V}_h$. Introducing this definition in equation (5), applying the inner product and assuming $\mathbf{r}(\boldsymbol{\varphi}) = \sum_j \mathbf{r}(\boldsymbol{\varphi}_j)\overline{N}_j(\mathbf{x})$, the problem reduces to a system of ordinary differential equations, $\forall j \in \overline{B} \backslash \overline{B}_D$:

$$\begin{cases} \partial_t \boldsymbol{\varphi}_j = \mathbf{r}(\boldsymbol{\varphi}_j), & \text{for } [t_n, t_{n+1/2}] \\ \boldsymbol{\varphi}_j(t_n) = \boldsymbol{\varphi}_{j,0} \end{cases} \tag{7}$$

with $\overline{B}$ the set of nodes of $\overline{\mathcal{T}}$, $\overline{B}_D$ the subset of nodes that belong to the Dirichlet boundary and $\overline{B} \backslash \overline{B}_D$ the complementary subset.

In order to integrate the reaction step, equation (7), it is not mandatory to construct the mesh $\overline{\mathcal{T}}$ or any field associated to this mesh. This can be avoided solving the system at each node of each mesh separatedly, using the interpolated value of all the others species at that node. For the interpolation, the value of the local coordinates of the nodes of a mesh correspondig to one specie in all the other computational meshes are needed. Local coordinates are computed before

the reactive step and saved. Each time that the value of any specie is needed it can be computed easely from these data.

The numerical scheme for the standard single-mesh strategy can be seen as a particular case of the previous formulation. Let $\mathcal{T}$ be the mesh that is shared for all species. Then, the mesh used to compute the reactive step, that contains all the different nodes of the set of meshes coincides with the mesh that is used for the transportation; that is $\overline{\mathcal{T}} = \bigcup_{i=1}^{n_e} \mathcal{T}_i = \mathcal{T}$. As a consequence, in the reactive step there is no need to interpolate any data and all the components of the solution of the ordinary systems of equations are used.

3 Adaptive algorithm

We use an adaptive scheme for time dependent problems based on [2]. There exist several algorithm to adapte the time step, for example [30]. In this work, only the spatial discretization is updated and the time step is kept constant in the whole simulation. The mesh adaptation process is done every m time steps. The first block of time steps is calculated until a convergence criteria is met (a global error indicator is lower than a tolerance and the number of nodes of two consecutive meshes is quite similar). This process is done in order reduce the error that arraise from the definition of the first computational mesh, that needs to be fine enought to capture the essential features of the solution [16] . The scheme is detailed in Algorithm 1, being $\mathbf{u}_{i,n}$ the solution of specie i at $t = n\Delta t$, and $\Delta t = m\delta t$ the remeshing time step and δt the integration time step.

Algorithm 1 Adaptive scheme without convergence control (except first Δt)

$\Delta t = m\delta t$
$\mathcal{T}^0 = \mathcal{T}^{ref}$
while No convergence **do**
  Compute the discret problem $[0, \Delta t]$ in $\{\mathcal{T}_i^0\}$
  Compute error indicator and generate the new set of meshes $\{\mathcal{T}_i^0\}$
end while
Save ($\mathbf{u}_{i,1}$,$\mathcal{T}_i^0$) for $i = 1, ..., n_e$
$n = 1$
$\mathcal{T}_i^n = \mathcal{T}_i^0$
while $n\Delta t < T$ **do**
  Compute the discret problem $[n\Delta t, (n+1)\Delta t]$ in $\{\mathcal{T}_i^n\}$
  Save ($\mathbf{u}_{i,(n+1)}$, $\mathcal{T}_i^n$) for $i = 1, ..., n_e$
  Compute error indicator and generate the new set of meshes $\{\mathcal{T}_i^{n+1}\}$
  Interpolate $\mathbf{u}_{i,n+1}$ to $\mathcal{T}_i^{n+1}$ for $i = 1, ..., n_e$
  $n = n + 1$
end while

The adaption of the mesh is based on remeshing a reference mesh with a maximum volume constraint imposed to its elements. The reference mesh should include an adequate description of the domain and common characteristics of all species. The maximum volume depends on the error indicator and the volumes of the elements of the previous computational mesh. It is imposed to the new elements of the mesh $\mathcal{T}_i^{n+1}$ that lies in the interior of the element r of the

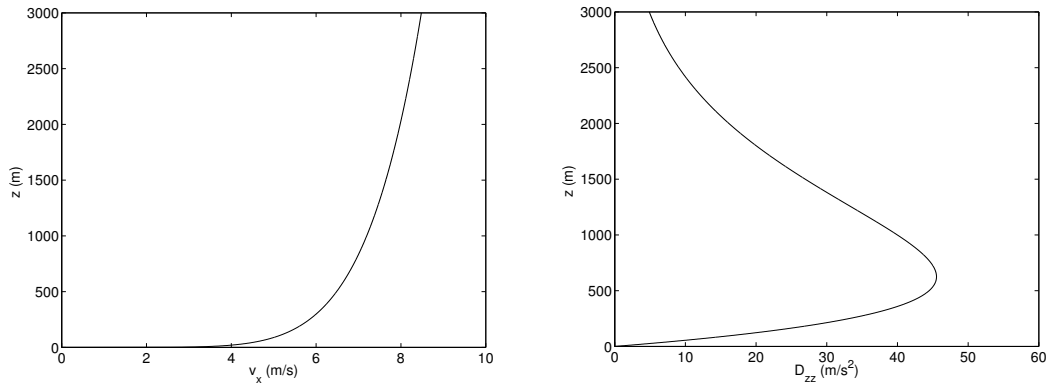

Figure 1: Vertical profile of the horizontal velocity modulus and the vertical diffusion.

mesh $\mathcal{T}^{ref}$. It is calculated as

$$V_{i,r}^{n+1} = \begin{cases} \min_{e \in S_{i,r}} \left(\frac{V_{i,e}}{1+\alpha \eta_{i,e}} \right) & \text{for } S_{i,r} \neq \emptyset \\ \beta V_{i,r}^{n} & \text{for } S_{i,r} = \emptyset \end{cases} \tag{8}$$

where $S_{i,r}$ are the subset of elements of the previous computational mesh, $\mathcal{T}_i^n$, that lies on the region r whose error indicator is larger than a tolerance, $\eta_{i,e}$ and $V_{i,e}$ are the error indicator and volume of element e of the specie i, and $\alpha > 0$ and $\beta > 1$ are two constants that modulate the refinement and the derrefinement, respectively. Further details of the implementation and a discussion of the values of the constants can be found in [17]. With this algorithm, the size of the elements can increase or decrease drastically in a single iteration. The quality of the meshes is preserved, and the number of iterations needed to solve the linear system of equations using an iterative method is kept low and constant. The meshes are constructed using $Tetgen$ [24, 25], a constrained Delaunay tetrahedral mesh generator.

For a single-mesh adaptive scheme, the computatinal meshes should be adapted to the most demanding specie in each part of the domain. The error indicator and the volume constraint are evaluated for all components of the solution. The new mesh is generated imposing the most restrictive volume constraint in each region:

$$V_r^{n+1} = \min_{1 \leq i \leq n_e} \left(\min_{e \in S_{i,r}} \left(\frac{V_{i,e}}{1+\alpha \eta_{i,e}} \right) \right) \tag{9}$$

if i exists such as $S_{i,r} \neq \emptyset$, and $V_r^{n+1} = \beta V_r^n$ if $S_{i,r} = \emptyset$ for all i.

The error is aproximated by an error indicator. In the literature there are several examples of error indicators for the convection-diffusion-reaction equation [13, 18]. This indicators are functions of the gradient or the maximum difference of the solution in the element. This kind of indicators are well suited to localize a boundary layer, but do not yeld good results for the point-source problem because the solution tends to be smooth in the domain and oscillations typicaly apear on the low values of the solution. A more adequate error indicator is:

$$\eta_\omega = \begin{cases} 0 & \text{if } u_h < Tol_u \text{ in } \omega \\ \| \nabla log(u_h) \|_\omega & \text{if } u_h > Tol_u \text{ in } \omega \end{cases} \tag{10}$$

where Tol_u defines the lower limit of the solution of which the mesh is no longer refined, typically a number related to the precision of the computer.

	Chemical elements	Species	emision rates ($\pi \cdot 10^2$ g/s)
Rivad-4	N, O, S	NO_x, NO_3, SO_2, SO_4^{2-}	$e_{SO_2} = \pi \cdot 10^4$; $e_{NO_x} = 2.5 \cdot \pi \cdot 10^3$
CB05-6	N, O	NO_2, NO, O, O_3, NO_3, N_2O_5	$e_{NO} = 6$; $e_O = 8$
CB05-15	N, O, H	NO_2, NO, O, O_3, NO_3, OH^-, HO_2, N_2O_5, HNO_3, HONO, PNA, H_2O_2, XO_2, ROOH, CH_2O	$e_{NO} = 6$; $e_O = 8$; $e_{OH^-} = 4$
CB05-29	N, O, H, C, Cl, S, free-radical	NO_2, NO, O, O_3, NO_3, OH^-, HO_2, N_2O_5, HNO_3, HONO, PNA, H_2O_2, XO_2, ROOH, CH_2O, CO, MEO_2, MEPX, MEO_2, FACD, SO_2, SO_4^{2-}, SULAER, Cl_2, Cl, HOCl, ClO, FACl, HCl	$e_{NO} = 6$; $e_O = 8$; $e_{OH^-} = 4$; $e_{SO_2} = 6$; $e_{CO} = 8$; $e_{Cl} = 4$

Table 1: Definition of the chemical mechanisms and the test examples.

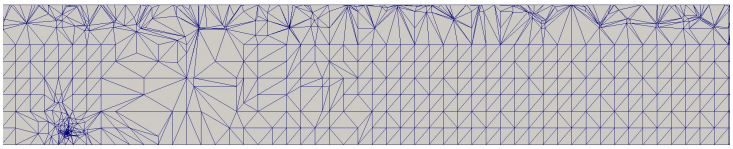

Figure 2: Reference mesh; profile at $y = 24000$ m.

4 Test examples

The proposal is applied to the test problem introduced in [11, 17]. It includes of a point source emission in a domain of size $\Omega = [0, 52000] \times [18000, 30000] \times [0, 3000]$ m^3. The punctual source is discretized with a sphere with radius $R = 5$ m. The meterological data corresponds to neutral conditions of [11, 23]. The convective velocity is parallel to the x-axis and its norm depends on height (see Figure 1). The diffusion tensor is diagonal and constant in the horitzontal plane, $D_{xx} = D_{yy} = 50$ m^2/s. The vertical component, D_{zz}, also depends on height (see Figure 1). First, both initial and inflow and outflow boundary conditions are set equal to zero. In next section, the problem is solved with all species, with realistic initial and boundary conditions. The emision rates, e_i, are given as a total point source value. They are applied to an emision sphere, Γ_{int}, with external surface A_{sph}

$$\mathbf{n} \cdot \mathbf{D} \cdot \nabla u_i = g_i(\mathbf{x}, t) = \frac{e_i}{A_{sph}} \text{ in } \Gamma_{int} \times (0, T) \tag{11}$$

The final integration time is $T = 1800$ s and the computational time-step is $\delta t = 1$ s. The mesh is adapted every $m = 180$ time-steps; that is $\Delta t = 180$s, ten remeshings. According to a previous work [17], a reduced number of remeshings minimices computational cost with appropiated accuracy. The same reference mesh, Figure 2, is used for all the species.

This problem is solved with different non-linear chemical models. The first one is the RIVAD/ARM3 model, wich involves four species. The second one is the CB05 photochemical model, the module implemented in CMAQ, wich involves sixty-two different unkowns. A set

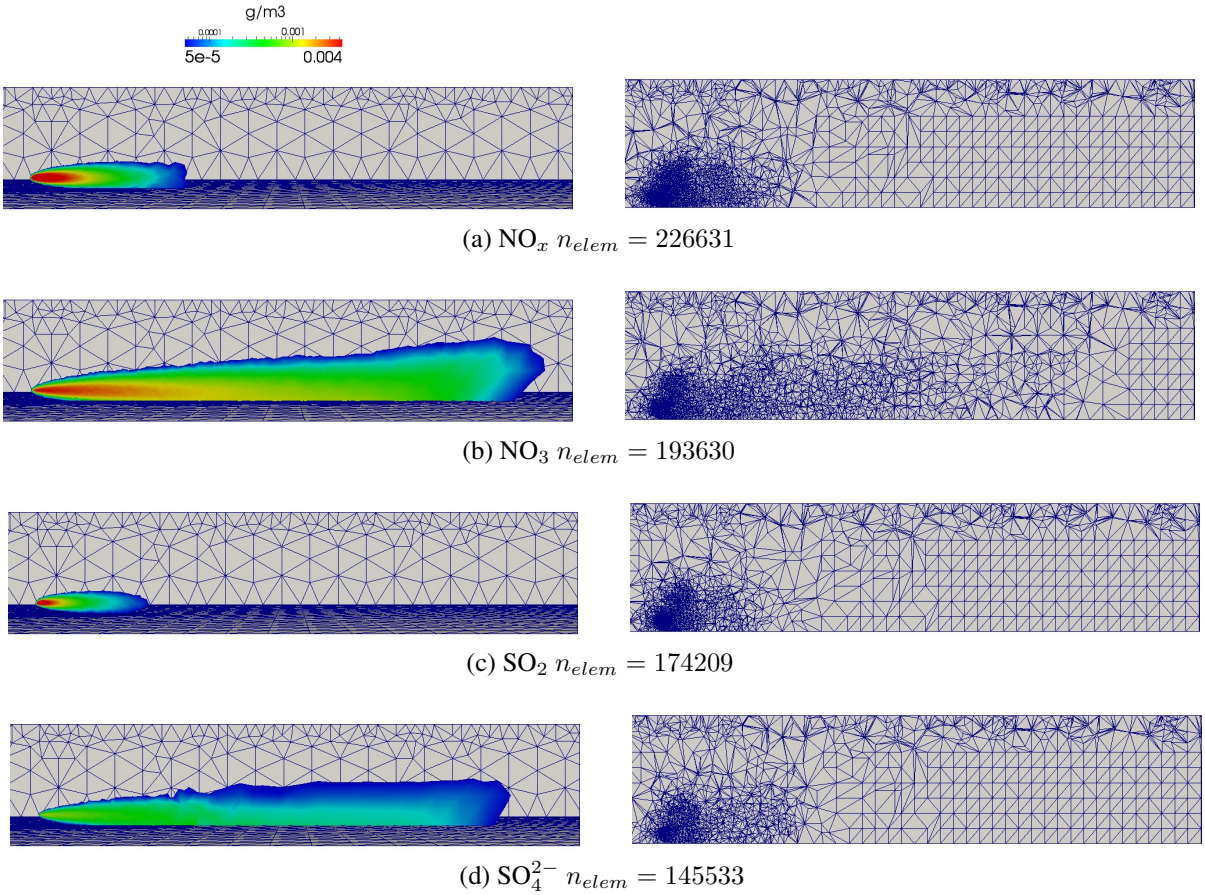

(a) NO_x $n_{elem} = 226631$

(b) NO_3 $n_{elem} = 193630$

(c) SO_2 $n_{elem} = 174209$

(d) SO_4^{2-} $n_{elem} = 145533$

Figure 3: Solution and mesh at $y = 24000$ m using the RIVAD chemical model, at $t = 1800$s. Primary pollutans, (a) and (c), and the secoundary ones, (b) and (d).

of test examples with the CB05 model has been defined, increasing the number of unknowns involved in transport, from 6 to 29. The species are chosed based on their chemical composition. The unkwon species are the ones that may be formed from a set of chemical species. The Table 1 shows the details of the species that involve each example and the emision rates.

4.1 RIVAD/ARM3 tests

The RIVAD/ARM3 scheme [21] is a simplified model that predicts the sulfate and nitrate production rate assuming a steady state concentration of the hydroxil radical. This model considers four especies and production rates are defined as [19]:

$$r_{\mathrm{SO_2}} = -r_{\mathrm{SO_4^{2-}}} = \alpha_1(\mathbf{u}) u_{\mathrm{SO_2}} = \frac{-\gamma_1}{u_{\mathrm{SO_2}} + \delta_1 u_{\mathrm{NO_x}}} u_{\mathrm{SO_2}} \tag{12a}$$

$$r_{\mathrm{NO_x}} = -r_{\mathrm{NO_3}} = \alpha_2(\mathbf{u}) u_{\mathrm{NO_x}} = \frac{-\gamma_2}{\delta_2 u_{\mathrm{SO_2}} + u_{\mathrm{NO_x}}} u_{\mathrm{NO_x}} \tag{12b}$$

where δ_1, δ_2, γ_1 and γ_2 are four constants. The initial and the inflow boundary conditions are zero for all species and the emision rate of the first primary pollutant is bigger than the second. A second-order method is used for time integration.

Figure 3 show the distribution of the primaries, Figures 3a and 3c, and the secondaries pollutants, Figures 3b and 3d. The primaries pollutant present the highest concentrations near the

source; they vanish forming the secondaries pollutants. The adaptive scheme can solve the problem without oscillations in the low values of the plume. The four meshes are different. Each one have small volumes in the regions where the solution presents high gradients. All the meshes have a small density of elements in the regions where the solution is very small (lower than 10^{-6}).

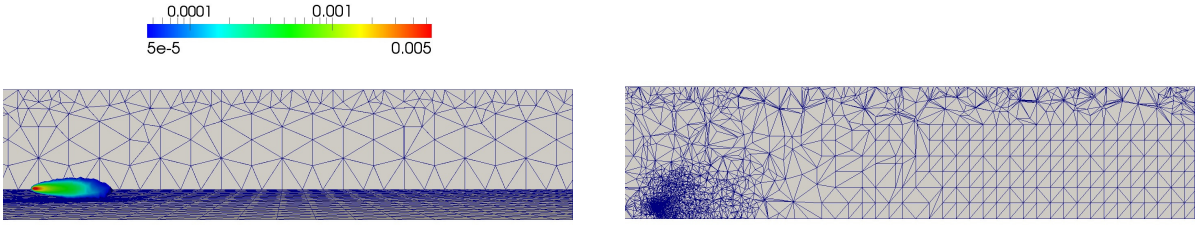

(a) NO_2; $n_{elem} = 165671$

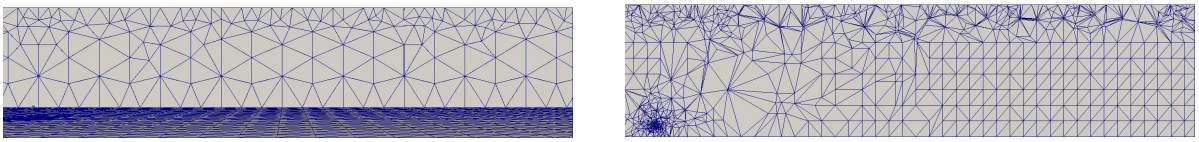

(b) NO; $n_{elem} = 124638$

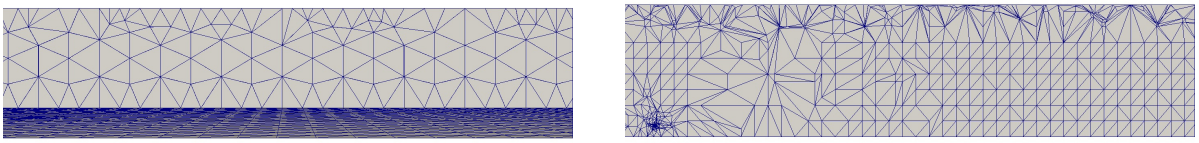

(c) O; $n_{elem} = 72192$

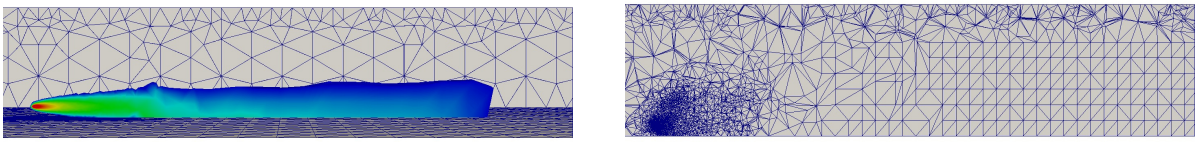

(d) O_3; $n_{elem} = 185936$

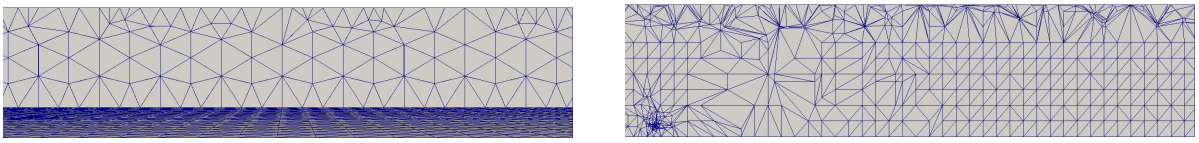

(e) NO_3; $n_{elem} = 72192$

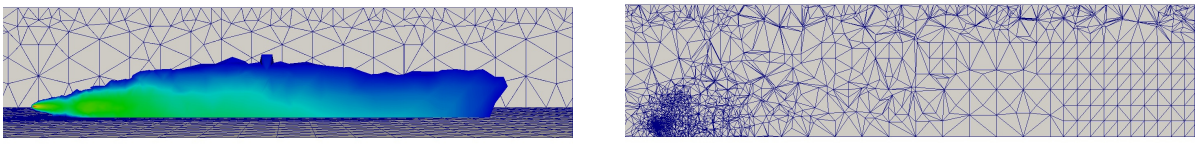

(f) N_2O_5; $n_{elem} = 147082$

Figure 4: The concentration, at $t = 1800$ s and $y = 24000$ m, of the CB05-6 test.

4.2 CB05 model tests

In the second example we have used the CMAQ chemical module [4], CB05, wich involves 62 species and 132 reactions. The EDOs sytem is solved using backwards Euler with an adaptive time step. The species of each case are choosen based on their elemental composition: The first example only involves Nitrogen and Oxigen (with $n_e = 6$ species, named CB05-06), the second one Nitrogen, Hidrogen and Oxigen (with $n_e = 15$, named CB05-15) and a third one Nitrogen, Hidrogen, Oxigen, Carbon, Clorine, Azufre y Raicales libres (with $n_e = 29$, named CB05-29).

Figure 4 shows the results with CB05-06 at $t = 1800$, for both primary pollutants, O and NO, which is practically zero near the source. This is because they react very fast and form O_3 and more oxidized nitrogen oxides. Ozone and some nitrogen oxides, NO_2 and N_2O_5, develop plumes. The concentration of NO_3 is practically zero in all the domain, thus the mesh used to compute it is very coarse. It can be seen that the meshes of all components are different. The volume of the elements is sufficiently small in the regions where the solution is not smooth and only small oscillations appear in the lowest isosurfaces. Some oscillations and numerical diffusion effects appear at low concentrations downwind at the end of the plumes, for example at the plume formed by NO_2 in Figure 4a. This process occurs in the transition of the refined mesh; it can be fixed with a more restrective tolerance for remeshing.

In the second test, CB05-15, the emited species, NO, O and OH^-, react forming different species involiving nitrogen (HONO, HNO_3, NO_2, ...), ozone and radicals. Six of the fifteen species develope different forms of plumes and the meshes are adapted to their form. In the last test, the main reactions that take place are the formation of components whose elementals components are Oxigen, Nitrogen, Hidrogen and Sulfur. Other species, for example the primary pollutant CO, are stable with this chemical conditions and do not react. Thirteen of the twenty-nine species develop a plume.

Table 2 summarizes main characteristics of all these examples: Number of degrees of freedoom at $t = 1800$ s, species which develope a plume, number of EDO solved, n_{EDO}, and total CPU time (s). The numbers of degrees of freedom and of species with a plume increase with the number of unknowns. The total number of EDO solved and CPU-time does not. First depends on the distribution of nodes between meshes. Rivad example involves more EDO than CB05 tests, even the number of unknowns is much higher. CPU time increases substantialy between CB05 and Rivad. This is because the standard chemical driver of CMAQ has been compiled with the transport code, without specific implementation adjustments; Rivad model is directly implented with the transport Finite Element Model. Within CB05 examples, CB05-06 and CB05-15 cases present a similar number of EDO and CPU-time (although the number of degrees of freedom doubles). CPU time doubles in last example, which doubles again in number of degrees of freedom (with respect to CB05-06 and CB05-15). Positive correlations beetwen the number of unknows, species, plumes and CPU-time are found, starting over an umbral value.

The results of three tests shows that all species are discretized in very different meshes. Acording to table 3, the number of nodes of the finner mesh is at least, two times the number of nodes of the coarser mesh. The species whose solution is low and smooth in the whole domain are discretized with very coarse meshes, even in the reference mesh. Instead, if the solution of one component develpes a plume, presenting high spatial variations of component concetration, it is discretized with a refined mesh. The density of elements is large where the solution present higher variantions (in orders of magnitude), trying to minimize spurios oscillations at very low

	n_{dof}	Species with plume	n_{EDO}	CPU-time (s)
Rivad single-mesh	194648	4	$2.29 \cdot 10^8$	3897
Rivad multi-mesh	146920	4	$2.74 \cdot 10^8$	3228 (83.05%)
CB05-6 single-mesh	220650	4	$1.625 \cdot 10^8$	12623
CB05-6 multi-mesh	158109	4	$1.823 \cdot 10^8$	12042 (95.40%)
CB05-15 single-mesh	580935	6	$1.6881 \cdot 10^8$	15374
CB05-15 multi-mesh	328406	6	$1.841 \cdot 10^8$	10952 (71.24%)
CB05-29 single-mesh	1083179	13	$1.6358 \cdot 10^8$	28192
CB05-29 multi-mesh	639854	13	$2.0974 \cdot 10^8$	19340 (68.61%)

Table 2: Comparison of the number of elements at $t = 1800$ s, CPU-time and total number of EDOs systems solved using multi-mesh and single-mesh schemes.

values. The number of species that develope plume is not know a priori, since it depends on the emisions, the concentration of all the other species, the meteorological conditions and the reaction rates. As a consequence, it is mandatory to take into account some species that have very low concentration (below 10^{-7}) just because they can potencially be formed.

Chemical model	min n_{nod} Multim	max n_{nod} Multi	n_{nod} Unimesh
Rivad	27070	41496	46726
CB05-6	16573	36648	36775
CB05-15	16573	36599	38729
CB05-29	16573	36125	37351

Table 3: Comparison of the number of nodes using the multi-mesh and single-mesh schemes at $t = 1800$ s.

4.3 Comparison of multi-mesh and single-mesh adaptive schemes

Four problems previously presented have been solved using the single-mesh scheme. The results obtained by both methods are very similar; the spurious oscillations that appear are of the same order. The size of the meshes using the single-mesh scheme is always similar to that of the most demanding specie of the multi-mesh scheme (see Table 3). Thus, the number of degrees of freedom is larger with the single-mesh scheme (see Table 2). Instead, the number of EDOs is larger with multi-mesh because the number of nodes uncommon between all meshes is also always larger than the size of one single mesh; see Table 3, with single-meshes more than two times the minimum multi-mesh one.

In the multi-mesh scheme all species are discretized in coarser meshes than with the single-mesh scheme. As a consequence, the CPU-time required for solving linear systems of equations decrease. However, this computation saving does not imply that the computational time of the whole simulation decrease. Using the multi-mesh scheme it is mandatory to compute the local coordinates of all nodes with respect all the other meshes, the number of EDOs solved is higher and more effor is needed in order to interpolate the solution every time the meshes are updated.

This extra work cause that not always the multi-mesh scheme suppose a CPU-time saving. Acording to Table 3, using the multi-mesh scheme the total CPU-time decrease with respect the single-mesh in all this examples. When an important number of components are discretized in very coarse meshes (CB05-15 and CB05-29, with 6 and 13 plumes), the improvement of multi-mesh is significant. If an important number of contaminants develope a plume (with respect the number of unknows), multi-mesh scheme could not represent a decrease of the computational time of the simulation.

5 Realistic example with CB05-CMAQ

The last example correspond to the same problem used as a test, but involving realistic values of initial and boundary conditions. Full CB05 model implemented within CMAQ system is used here, coupled with the Finite Element transport solver adn main driver. Non-zero Dirichlet boundary conditions are imposed in the inflow, same as initial values of all species in the domain. Values of concentrations varies on height, being uniform in the plane coordinates. Values are interpolated in a certain point from a CMAQ realistic simulation. The composition of the emission is a simplified version of a coal power plant [1, 8]:

$$e_i = \begin{cases} 2.71 \cdot \pi \cdot 10^3 \text{ g/s} & \text{if } i = \text{SO}_2 \\ 2.21 \cdot \pi \cdot 10^3 \text{ g/s} & \text{if } i = \text{NO} \\ 2.37 \cdot \pi \cdot 10^3 \text{ g/s} & \text{if } i = \text{CO} \\ 0 \text{ g/s} & \text{all the others} \end{cases} \tag{13}$$

Unlike data in the CMAQ simulation, here, the temperature, humidity and preasure (on which the reactions rate deppends) are suposed to be constant in the whole domain, and values are linearly interpolated between CMAQ altitudes. Those are reasons why at the begining of the simulation, the background concentrations varies; until a new equilibrium is reached. These reactions also preclude gradients in some species near the Dirichlet inflow boundary (which are kept fixed).

Figure 5 shows the concentration of some representative species. As it can be seen, the backgroud concentration of the majority of species is very low (below 10^{-7}) and with smooth variantions in all the domain. Their computational meshes are not refined, reference mesh is used, for example, with HNO_3 in Figure 5f. Some species have relative high background concentrations, even they present layers. As a consequence, some refinement are activated to represent the vertical variation; this is the case of ozone and CO in Figure 5c. The main reaction that takes place is the formation of NO_2 form the background ozone and emitted NO. This reaction takes place until the avalaible ozone is consumed. The mesh in which ozone is discretized, Figure 5e, is refined in the zones where the concentration presents large gradients. A similar behavior is observed for CO. The interactions of CO and SO_2, two of the primary pollutans, with the others species are low; both species develope plume.

6 Conclusions

In this paper, we have presented an adaptive multi-mesh scheme for the reactive transport problem, using the Finite Element method. Each component of the solution is discretized on an individual mesh, that is independently adapted based on the evolution of its solution. The proposal has been succesfully applied to a set of tests of increasing number of unknowns and complexity of a punctual source emissor with realistic atmospheric and air quality conditions

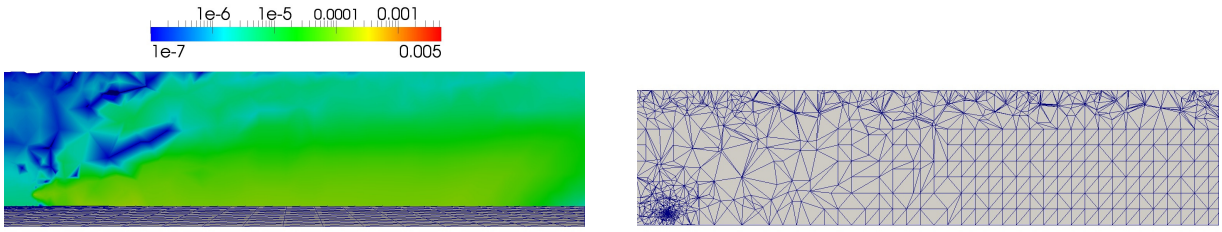

(a) NO_2; $n_{elem} = 125025$

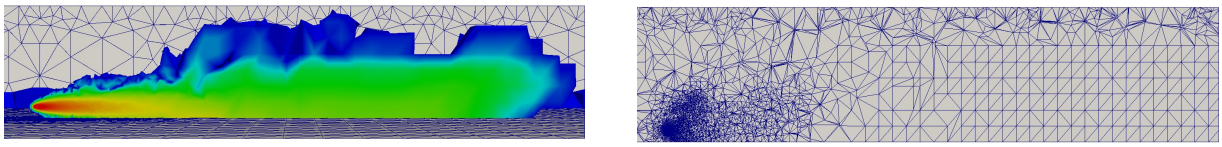

(b) NO; $n_{elem} = 198079$

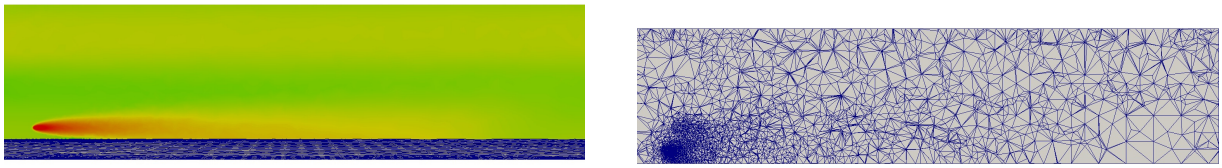

(c) CO; $n_{elem} = 588565$

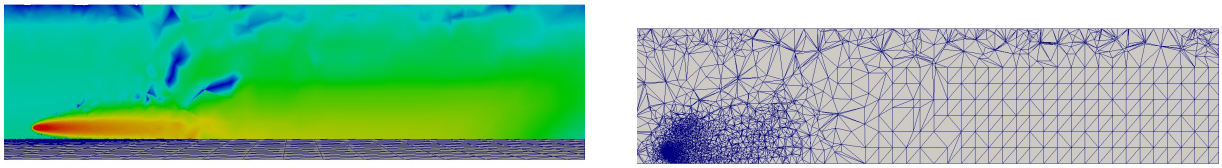

(d) SO_2; $n_{elem} = 201733$

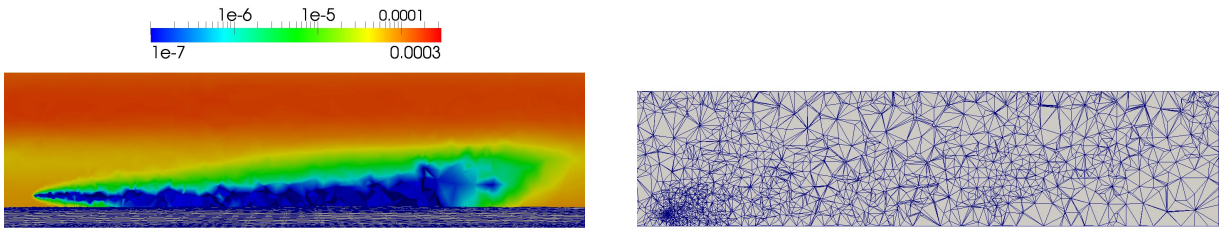

(e) O_3; $n_{elem} = 402440$

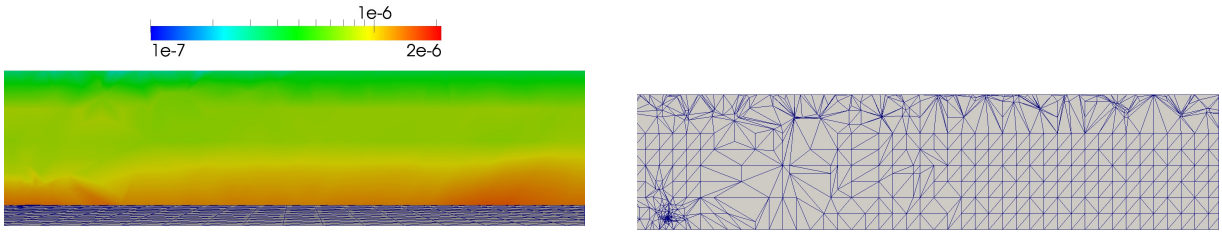

(f) HNO_3; $n_{elem} = 72912$

Figure 5: The concentration, at $t = 1800$, of some pollutants of the CB05-62 test at $y = 24000$ m.

in a three-dimensional domain. The CB05 photochemical model has been used, with the same implementation provided with the CMAQ system.

The proposal solves the problem with the same accuracy than a single-mesh adaptive method. The computational cost of the multi-mesh scheme is, in general, lower than the standard single-mesh scheme. Time saving is more important when only few species develope plume, thus, with meshes refined and adapted, and the most ones vary smoothly through the domain, being discretized in coarse meshes. Work needed for multi-mesh discretization is not always smaller than the time saving given by the smaller systems of equations obtained.

Acording to the results, the adaptive multi-mesh schemes are capable of using less degrees of freedom to achieve the same accuray than a standard single-mesh adaptive method. The size of the mesh of the most demanding specie with the multi-mesh scheme is of the same order than the one obtained with the single-mesh approach. But most species, specially the ones that do not present large variation in the space, are discretized in coarse meshes, of much smaller size. Thus, less unknows are involved; however, the number of differents nodes in the overall meshes is larger and more systems of EDOs have to be computed.

Strategy can be applied either with a single-mesh a multi-mesh, or even a fixed number of meshes if unknowns are asigned to each mesh; and optimal stratgies can be defined in terms of computational resources. Problems with large number of species, developing different spatial patterns, are more efficiently solved with multi-mesh strategies.

REFERENCES

[1] European Environment Agency. Air pollution from electricity-generating large combustion plants. *EEA Technical report*, 4, 2008.

[2] F. Alauzet, P.L. George, B. Mohammadi, P. Frey, and H. Borouchaki. Transient fixed point-based unstructured mesh adaptation. *International journal for numerical methods in fluids*, 43(6-7):729–745, 2003.

[3] V.N. Alexandrov, W. Owczarz, P.G. Thomson, and Z. Zlatev. Parallel runs of a large air pollution model on a grid of Sun computers. *Mathematics and Computers in Simulation*, 65(6):557–577, 2004.

[4] D.W. Byun and J.K.S. Ching. *Science algorithms of the EPA Models-3 community multiscale air quality CMAQ modeling system*. US Environmental Protection Agency, Office of Research and Development, 1999.

[5] A. Chertock, A. Kurganov, and G. Petrova. Fast explicit operator splitting method for convection–diffusion equations. *International Journal for Numerical Methods in Fluids*, 59(3):309–332, 2009.

[6] J. Donea and A. Huerta. *Finite Element Methods for Flow Problems*. Wiley Online Library, 2003.

[7] L. Dubcova, P. Solin, J. Cerveny, and P. Kus. Space and time adaptive two-mesh hp-FEM for transient microwave heating problems. *Electromagnetics*, 30(1):23–40, 2010.

[8] GJ Frost, SA McKeen, M. Trainer, TB Ryerson, JA Neuman, JM Roberts, A. Swanson, JS Holloway, DT Sueper, T. Fortin, et al. Effects of changing power plant nox emissions on ozone in the eastern united states: Proof of concept. *J. Geophys. Res*, 111(D12):D21306, 2006.

[9] F. Garcia-Menendez and M.T. Odman. Adaptive grid use in air quality modeling. *Atmosphere*, 2(3):484–509, 2011.

[10] F. Garcia-Menendez, A. Yano, Y. Hu, and MT Odman. An adaptive grid version of CMAQ for improving the resolution of plumes. *Atmospheric Pollution Research*, 1:239–249, 2010.

[11] S. Ghorai, AS Tomlin, and M. Berzins. Resolution of pollutant concentrations in the boundary layer using a fully 3D adaptive gridding technique. *Atmospheric Environment*, 34(18):2851–2863, 2000.

[12] X. Hu, R. Li, and T. Tang. A multi-mesh adaptive finite element aproximation to phase field models. *Communications in Computational Physics*, 5(5):1012–1029, 2009.

[13] V. John. A numerical study of a posteriori error estimators for convection–diffusion equations. *Computer methods in applied mechanics and engineering*, 190(5):757–781, 2000.

[14] R. Li. On multi-mesh h-adaptive methods. *Journal of Scientific Computing*, 24(3):321–341, 2005.

[15] C.J. Lin and J.J. Moré. Incomplete Cholesky factorizations with limited memory. *SIAM Journal on Scientific Computing*, 21(1):24–45, 2000.

[16] M. Möller and D. Kuzmin. Adaptive mesh refinement for high-resolution finite element schemes. *International journal for numerical methods in fluids*, 52(5):545–569, 2006.

[17] L. Monforte and A. Pérez-Foguet. Un esquema adaptativo para problemas tridimensionales de convección – difusión/ An adaptive scheme for convection – difussion problems in three-dimensions. *Revista Internacional de Métodos Numéricos para Cálculo y Diseño en Ingeniería, accepted*, 2012.

[18] R. Montenegro, G. Montero, G. Winter, and L. Ferragut. Aplicación de métodos de elementos finitos adaptativos a problemas de convección-difusión. *Reo. Int. Met. Num. Cal. y Dis. en Ing*, 5(4):535–560, 1989.

[19] A. Oliver, G. Montero, R. Montenegro, E. Rodríguez, J.M. Escobar, and A. Pérez-Foguet. Adaptive finite element simulation of air pollution over complex terrains. *Advances in Science and Research*, 8:105–113, 2012.

[20] A. Rodríguez-Ferran and M.L. Sandoval. Numerical performance of incomplete factorizations for 3D transient convection–diffusion problems. *Advances in Engineering Software*, 38(6):439–450, 2007.

[21] J.S. Scire, D.G. Strimaitis, and R.J. Yamartino. A users guide for the CALPUFF dispersion model. *Earth Tech, Inc*, 521, 2000.

[22] C. Seigneur. Air pollution: current challenges and future opportunities. *AIChE journal*, 51(2):356–364, 2005.

[23] J.H. Seinfeld. *Atmospheric chemistry and physics of air pollution*. John Wiley and Sons, Inc., Somerset, NJ, 1986.

[24] H. Si. On refinement of constrained Delaunay tetrahedralizations. In *Proceedings of the 15th international meshing roundtable*, pages 61–69. Citeseer, 2006.

[25] H. Si. Constrained Delaunay tetrahedral mesh generation and refinement. *Finite elements in Analysis and Design*, 46(1):33–46, 2010.

[26] P. Solin, J. Cerveny, L. Dubcova, and D. Andrs. Monolithic discretization of linear thermoelasticity problems via adaptive multimesh hp-FEM. *Journal of computational and applied mathematics*, 234(7):2350–2357, 2010.

[27] P. Solin, L. Dubcova, and J. Kruis. Adaptive hp-FEM with dynamical meshes for transient heat and moisture transfer problems. *Journal of computational and applied mathematics*, 233(12):3103–3112, 2010.

[28] RK Srivastava, DS McRae, and MT Odman. Simulation of dispersion of a power plant plume using an adaptive grid algorithm. *Atmospheric Environment*, 35(28):4801–4818, 2001.

[29] A.S. Tomlin, S. Ghorai, G. Hart, and M. Berzins. 3d adaptive unstructured meshes for air pollution modelling. *Environmental Management and Health*, 10(4):267–275, 1999.

[30] A.M.P. Valli, G.F. Carey, and A.L.G.A. Coutinho. Control strategies for timestep selection in finite element simulation of incompressible flows and coupled reaction–convection–diffusion processes. *International journal for numerical methods in fluids*, 47(3):201–231, 2005.

[31] A. Voigt and T. Witkowski. A multi-mesh finite element method for Lagrange elements of arbitrary degree. *Preprint*, 2010.

[32] Y.X. Wang, M.B. McElroy, D.J. Jacob, and R.M. Yantosca. A nested grid formulation for chemical transport over asia: Applications to CO. *J. Geophys. Res*, 109:D22307, 2004.